

State Change via One-Dimensional Scattering in Quantum Mechanics

Olivia Pomerenk and Charles S. Peskin

June 2025

Abstract

We consider a pair of particles that interact in a one-dimensional setting via a delta-function potential. One of the particles is confined to a one-dimensional box, and the other particle is free. The free particle is incident from the left with specified energy, and it may cause changes in state of the confined particle before flying away to the left or to the right. We present a non-perturbative formulation and computational scheme that determines the probability of any such outcome, as a function of the initial state of the confined particle and the energy of the incident particle.

1 Introduction

Quantum mechanics gets its name from the observed discreteness of the states of quantum systems, and such observations always involve transitions between states. In atomic physics, for example, the energy levels of atoms are observed by means of spectroscopy, in which photons are emitted or absorbed and the changes in energy level are thereby inferred. The description of this particular process requires quantum electrodynamics, however, which is beyond the scope of the present paper.

In ordinary non-relativistic quantum mechanics, changes in the state of a system can be brought about via interaction with another system, and the mathematical framework for studying such changes is time-dependent perturbation theory. There is something peculiar about this procedure, however, which can be brought out by considering the composite system as a system in its own right. Like any quantum-mechanical system, the composite system has a spectrum of stationary states, and its most general state is a superposition of its stationary states. Such a superposition is characterized by amplitudes c_k , and the physically important quantities are $|c_k|^2$, which do not change with time. Thus, from the point of view of the composite system, nothing is happening! How can it be, then, that the interaction with another system is causing changes in the state of the original system? The answer to this question requires the theory of measurement. After the interaction between the two systems has taken place for some time, we can measure some property

of the original system, and may find that it has changed. It is the probability of such a change that is calculated by time-dependent perturbation theory.

In the present paper we consider a particularly simple example of state change via scattering, in which the measurement step is essentially built into the interaction process, and in which we are able to compute the probabilities of a finite number of different possible outcomes without resort to any kind of perturbation theory. This is done by formulating the problem as an infinite system of integral equations, which are solved numerically with second-order accuracy. This approach thus differs from that of previous works, e.g., [4], in which time-dependent perturbation theory is used to characterize the effect of an external non-autonomous perturbation on a bound state. This work instead treats the composite system (external system interacting with a bound state) altogether.

In one spatial dimension, we consider a two-particle system. One of the particles is confined to a box (i.e., an interval) of length L , but the walls of the box are transparent to the other particle, which moves freely on the whole real line. The two particles interact via a delta-function potential, which may be attractive or repulsive. In the scattering problem that we consider, there is an incoming state, in which the free particle is incident from the left with a definite energy, and the confined particle is in a particular stationary state of a particle in a one-dimensional box. This incoming state is a product state of the wavefunctions of the two particles, which means that the particles are independent in the distant past, before any interaction has occurred. The outgoing state is *not* a product state, however. The interaction has correlated the states of the two particles, so that observation of the outgoing state of the free particle determines the corresponding state of the confined particle (assuming that the incoming states were known).

2 Problem statement

We consider scattering in one spatial dimension by a local interaction between two particles, with one particle free and the other confined to a one-dimensional (1D) box. The particles respectively have mass m_1 and m_2 . The particle with mass m_2 is confined to the interval $(0, L)$, while the particle with mass m_1 is free.

The configuration space of the system is

$$\mathbb{R} \times (0, L), \tag{1}$$

and the time-independent Schrödinger equation is

$$-\frac{\hbar^2}{2m_1} \frac{\partial^2 \Psi}{\partial x_1^2} - \frac{\hbar^2}{2m_2} \frac{\partial^2 \Psi}{\partial x_2^2} + \mu_0 \delta(x_1 - x_2) \Psi = E \Psi \tag{2}$$

with boundary conditions

$$\Psi(x_1, 0) = \Psi(x_1, L) = 0. \tag{3}$$

The constant $\mu_0 \in \mathbb{R}$ has units of energy \cdot length. Positive $\mu_0 > 0$ is associated with a repulsive interaction potential, while negative $\mu_0 < 0$ is associated with an attractive

interaction potential. The interaction takes place along the line $x_1 = x_2$ in configuration space.

Let

$$\phi_n(x_1) = \int_0^L \sin\left(\frac{n\pi x_2}{L}\right) \Psi(x_1, x_2) dx \quad (4)$$

$$\Psi(x_1, x_2) = \frac{2}{L} \sum_{n=1}^{\infty} \sin\left(\frac{n\pi x_2}{L}\right) \phi_n(x_1) \quad (5)$$

be a Fourier decomposition of the wavefunction Ψ such that the boundary conditions (3) are satisfied by (5). To get an equation for $\phi_n(x_1)$, we multiply both sides of (2) by $\sin(n\pi x_2/L)$ and, making use of (5), integrate with respect to x_2 over $(0, L)$. This yields

$$-\frac{\hbar^2}{2m_1} \frac{d^2 \phi_n}{dx^2}(x) + \frac{\hbar^2}{2m_2} \left(\frac{n\pi}{L}\right)^2 \phi_n(x) + \frac{2\mu_0}{L} C(x) \sin\left(\frac{n\pi x}{L}\right) \sum_{n'=1}^{\infty} \sin\left(\frac{n'\pi x}{L}\right) \phi_{n'}(x) = E \phi_n(x) \quad (6)$$

where we have simplified the notation by writing $x = x_1$, as the integration with respect to x_2 has removed all dependencies on x_2 . Here,

$$C(x) = \begin{cases} 1, & x \in (0, L) \\ 0, & x \notin (0, L). \end{cases} \quad (7)$$

We seek a solution to (6) in the form

$$\phi_n(x) = \delta_{nn_0} e^{ik_0 x} + \Phi_n(x) \quad (8)$$

in which $\Phi_n(x)$ involves only outgoing waves or decays exponentially as $|x| \rightarrow \infty$.

Here, n_0 corresponds to the index of the stationary state of the confined particle in the 1D box, and k_0 is the wavenumber of the incident free particle. This particular form (8) is chosen to represent the composite state of the incoming wave and the confined particle as a product state, as the two sub-systems must be independent. This product state takes the form $e^{ik_0 x_1} \sin(n_0 \pi x_2 / L)$, which has the interpretation that the free particle (with coordinate x_1) is in a state of definite momentum and energy and is completely de-localized, while the confined particle (with coordinate x_2) is in the stationary state with index n_0 of a particle in a 1D box. The Fourier transform with respect to x_2 of this product state is $\delta_{nn_0} e^{ik_0 x}$, which is the form given above. Thus, there is no correlation between the particles in the incoming state, but correlation may be generated by the interaction in the outgoing state.

We require that the term $\delta_{nn_0} e^{ik_0 x}$ be a solution to (6) for $x \notin (0, L)$. This implies that the total energy is

$$E = \frac{\hbar^2}{2m_1} k_0^2 + \frac{\hbar^2}{2m_2} \left(\frac{n_0 \pi}{L}\right)^2. \quad (9)$$

Thus, (6) becomes

$$\begin{aligned}
& -\frac{\hbar^2}{2m_1} \frac{d^2 \Phi_n}{dx^2}(x) + \frac{\hbar^2}{2m_2} \left(\frac{n\pi}{L} \right)^2 \Phi_n(x) \dots \\
& + \frac{2\mu_0}{L} C(x) \sin\left(\frac{n\pi x}{L}\right) \sum_{n'=1}^{\infty} \sin\left(\frac{n'\pi x}{L}\right) (\delta_{n'n_0} e^{ik_0 x} + \Phi_{n'}(x)) = E\phi_n(x).
\end{aligned} \tag{10}$$

Multiplying both sides of (10) by $2m_1/\hbar^2$ and making use of (9) yields

$$\begin{aligned}
& -\frac{d^2 \Phi_n}{dx^2}(x) + \left(\frac{m_1}{m_2} \left(\frac{\pi}{L} \right)^2 (n^2 - n_0^2) - k_0^2 \right) \Phi_n(x) \\
& = -\frac{4m_1\mu_0}{\hbar^2 L} C(x) \sin\left(\frac{n\pi x}{L}\right) \sum_{n'=1}^{\infty} \sin\left(\frac{n'\pi x}{L}\right) (\delta_{n'n_0} e^{ik_0 x} + \Phi_{n'}(x)).
\end{aligned} \tag{11}$$

Let

$$a_n = \frac{m_1}{m_2} \left(\frac{\pi}{L} \right)^2 (n^2 - n_0^2) - k_0^2, \quad n = 1, 2, \dots \tag{12}$$

Then $a_1 < 0$ and $a_n > 0$ for sufficiently large n . We assume that $\nexists n$ such that $a_n = 0$. Next, define

$$k_n = \sqrt{-a_n}, \quad a_n < 0 \tag{13}$$

$$\lambda_n = \sqrt{a_n}, \quad a_n > 0. \tag{14}$$

For n such that $a_n < 0$, introduce the Green's function

$$G_n(x) = -\frac{1}{2ik_n} \begin{cases} e^{-ik_n x}, & x < 0 \\ e^{ik_n x}, & x > 0 \end{cases} \tag{15}$$

and for n such that $a_n > 0$, define

$$G_n(x) = \frac{1}{2\lambda_n} \begin{cases} e^{\lambda_n x}, & x < 0 \\ e^{-\lambda_n x}, & x > 0. \end{cases} \tag{16}$$

Then, for all $n = 1, 2, \dots$, G_n satisfies

$$-\frac{d^2 G_n}{dx^2}(x) + a_n G_n(x) = \delta(x). \tag{17}$$

It follows by linearity that (11) may be written as

$$\Phi_n(x) = -\frac{4m_1\mu_0}{\hbar^2 L} \int_0^L G_n(x-x') \sin\left(\frac{n\pi x'}{L}\right) \sum_{n'=1}^{\infty} \sin\left(\frac{n'\pi x'}{L}\right) (\delta_{n'n_0} e^{ik_0 x'} + \Phi_{n'}(x')) dx'. \tag{18}$$

Defining

$$A_{nn'}(x) = \frac{4m_1\mu_0}{\hbar^2 L} \sin\left(\frac{n\pi x}{L}\right) \sin\left(\frac{n'\pi x}{L}\right), \quad (19)$$

this becomes

$$\Phi_n(x) + \sum_{n'=1}^{\infty} \int_0^L G_n(x-x') A_{nn'}(x') \Phi_{n'}(x') dx' = - \int_0^L G_n(x-x') A_{nn_0}(x') e^{ik_0 x'} dx'. \quad (20)$$

This is a system of Fredholm integral equations of the second kind.

3 Interpretation of results

Assuming that we can solve (20), we discuss in this section a physical interpretation of the solution $\Phi_n(x)$. First, consider the formulation of probability flux, which is derived for the time-dependent Schrödinger equation,

$$i\hbar \frac{\partial \Psi}{\partial t} = -\frac{\hbar^2}{2m_1} \frac{\partial^2 \Psi}{\partial x_1^2} - \frac{\hbar^2}{2m_2} \frac{\partial^2 \Psi}{\partial x_2^2} + \mu_0 \delta(x_1 - x_2) \Psi. \quad (21)$$

Manipulation of (21) yields

$$\frac{\partial}{\partial t} |\Psi|^2 + \frac{\partial}{\partial x_1} \frac{\hbar}{2im_1} \left(\bar{\Psi} \frac{\partial \Psi}{\partial x_1} - \Psi \frac{\partial \bar{\Psi}}{\partial x_1} \right) + \frac{\partial}{\partial x_2} \frac{\hbar}{2im_2} \left(\bar{\Psi} \frac{\partial \Psi}{\partial x_2} - \Psi \frac{\partial \bar{\Psi}}{\partial x_2} \right) = 0, \quad (22)$$

which has the form of a continuity equation, i.e.,

$$\frac{\partial \rho}{\partial t} + \frac{\partial f_1}{\partial x_1} + \frac{\partial f_2}{\partial x_2} = 0 \quad (23)$$

where

$$\rho = |\Psi|^2 \quad (24)$$

$$f_1 = \frac{\hbar}{2im_1} \left(\bar{\Psi} \frac{\partial \Psi}{\partial x_1} - \Psi \frac{\partial \bar{\Psi}}{\partial x_1} \right) \quad (25)$$

$$f_2 = \frac{\hbar}{2im_2} \left(\bar{\Psi} \frac{\partial \Psi}{\partial x_2} - \Psi \frac{\partial \bar{\Psi}}{\partial x_2} \right). \quad (26)$$

In particular, if Ψ has time dependence $e^{-i\omega t}$, then this time dependence cancels out of the above.

Define the integral of the flux associated with particle 1,

$$F(x_1) = \int_0^L f_1(x_1, x_2) dx_2. \quad (27)$$

To evaluate $F(x_1)$, we make use of (5) and (25) to obtain

$$\overline{\Psi} \frac{\partial \Psi}{\partial x_1} = \left(\frac{2}{L}\right)^2 \sum_{n,n'=1}^{\infty} \sin\left(\frac{n\pi x_2}{L}\right) \sin\left(\frac{n'\pi x_2}{L}\right) \overline{\phi_{n'}(x_1)} \frac{\partial \phi_n}{\partial x_1}(x_1). \quad (28)$$

Integrating both sides of (28) over $(0, L)$ with respect to x_2 removes the dependence on x_2 , and so we again drop the subscript 1 on x for ease of notation. We obtain

$$F(x) = \frac{\hbar}{2im_1} \frac{2}{L} \sum_{n=1}^{\infty} \left(\overline{\phi_n(x)} \frac{d\phi_n}{dx}(x) - \phi_n(x) \overline{\frac{d\phi_n}{dx}(x)} \right). \quad (29)$$

Note the absence of interference terms between different n .

For $x > L$, we write

$$\phi_n(x) = \begin{cases} \phi_n(L) e^{ik_n(x-L)} & a_n < 0 \\ \phi_n(L) e^{-\lambda_n(x-L)} & a_n > 0. \end{cases} \quad (30)$$

Then, for n such that $a_n > 0$,

$$\overline{\phi_n(x)} \frac{d\phi_n}{dx}(x) - \phi_n(x) \overline{\frac{d\phi_n}{dx}(x)} = 0. \quad (31)$$

Substitution of (30) into (29) therefore implies that, for $x > L$,

$$F(x) = \frac{2}{L} \sum_{n:a_n < 0} \frac{\hbar k_n}{m_1} |\phi_n(L)|^2 = \frac{2}{L} \sum_{n:a_n < 0} \frac{\hbar k_n}{m_1} |\Phi_n(L) + \delta_{nn_0} e^{ik_0 L}|^2. \quad (32)$$

For $x < 0$ and $n \neq n_0$, a similar argument holds with $k_n \rightarrow -k_n$, $\lambda_n \rightarrow -\lambda_n$, and $\phi_n(L) \rightarrow \phi_n(0)$. For the particular case of $n = n_0$ and $x < 0$, we have

$$\phi_{n_0}(x) = e^{ik_0 x} + \Phi_{n_0}(0) e^{-ik_0 x} \quad (33)$$

and so

$$F(x) = \frac{2}{L} \frac{\hbar k_0}{m_1} - \frac{2}{L} \sum_{n:a_n < 0} \frac{\hbar k_n}{m_1} |\Phi_n(0)|^2. \quad (34)$$

Note that $F(x)$ is independent of x , which implies conservation of probability.

We see that $2\hbar k_0/Lm_1$ is the incoming flux of probability, so we divide $F(x)$ by this and make the definitions

$$p_n^+ = \frac{k_n}{k_0} |\Phi_n(L) + \delta_{nn_0} e^{ik_0 L}|^2 \quad (35)$$

$$p_n^- = \frac{k_n}{k_0} |\Phi_n(0)|^2 \quad (36)$$

for n such that $a_n < 0$. Here, p_n^+ is the probability that particle 1 exits to the right with wavenumber k_n , leaving particle 2 in the n^{th} stationary state of a particle in a box, and p_n^- is the probability that particle 1 exits to the left, leaving particle 2 in the n^{th} stationary state. The total probability that particle 2 is in stationary state n as a consequence of the interaction is thus

$$p_n = p_n^+ + p_n^-. \quad (37)$$

3.1 Restriction to finitely many outcomes

There are a finite number of possible outcomes of (35) and (36) due to the restriction $a_n < 0$. Each of the different outcomes conserve energy. The energy of the incoming state, by (9), is

$$E_0 = \frac{\hbar^2}{2m_1} k_0^2 + \frac{\hbar^2}{2m_2} \left(\frac{n_0 \pi}{L} \right)^2. \quad (38)$$

The energy for either of the states n (i.e., with particle 1 exiting to the right or left while leaving particle 2 in the n^{th} stationary state) is

$$E_n = \frac{\hbar^2}{2m_1} k_n^2 + \frac{\hbar^2}{2m_2} \left(\frac{n \pi}{L} \right)^2. \quad (39)$$

Substituting (12) and (13) into the above yields $E_n = E_0$.

Further, it must be the case that

$$\sum_{n: a_n < 0} (p_n^+ + p_n^-) = \sum_{n: a_n < 0} p_n = 1. \quad (40)$$

This is an immediate consequence of the fact that $F(x)$ is independent of x : equating the right hands sides of (32) and (34) gives an equation which may be manipulated to produce (40).

In the next section, we present a method with which to solve (20) numerically for $\Phi_n(x)$ on the interval $[0, L]$, and to thus compute the transmission and reflection probabilities given by (35) and (36).

4 Numerical method

We seek to solve (20) for $\Phi_n(x)$ with $n = 1, \dots, T$ on the interval $x \in [0, L]$. First, denote the right hand side of (20) by

$$f_n(x) = - \int_0^L G_n(x - x') A_{nn_0}(x') e^{ik_0 x'} dx', \quad (41)$$

which is known for $x \in [0, L]$. Equation (20) may be written as a system of T equations:

$$\begin{aligned} \Phi_1(x) + \sum_{n'=1}^{\infty} \int G_1(x - x') A_{1n'}(x') \Phi_{n'}(x') dx' &= f_1(x) \\ \Phi_2(x) + \sum_{n'=1}^{\infty} \int G_2(x - x') A_{2n'}(x') \Phi_{n'}(x') dx' &= f_2(x) \\ &\vdots \\ \Phi_T(x) + \sum_{n'=1}^{\infty} \int G_T(x - x') A_{Tn'}(x') \Phi_{n'}(x') dx' &= f_T(x). \end{aligned} \quad (42)$$

In order to make this a system of T equations for T unknowns, and thus uniquely determine $\Phi_n(x)$, we must truncate the infinite series within each equation at $n' = T$:

$$\begin{aligned}
\Phi_1(x) + \sum_{n'=1}^T \int G_1(x-x') A_{1n'}(x') \Phi_{n'}(x') dx' &= f_1(x) \\
\Phi_2(x) + \sum_{n'=1}^T \int G_2(x-x') A_{2n'}(x') \Phi_{n'}(x') dx' &= f_2(x) \\
&\vdots \\
\Phi_T(x) + \sum_{n'=1}^T \int G_T(x-x') A_{Tn'}(x') \Phi_{n'}(x') dx' &= f_T(x).
\end{aligned} \tag{43}$$

So long as T is sufficiently large, this truncation should be appropriate for $x \in [0, 1]$. This is because, by (15) and (16), the quantity $G_n(x)$ decays exponentially as $n \rightarrow \infty$ for any $x \in \mathbb{R}$. Thus, $|\Phi_n(x)| \rightarrow 0$ for all x .

Now we discretize equations (43) using N equally spaced quadrature nodes $\{x_1, \dots, x_N\}$ on $[0, L]$ such that $x_1 = 0$ and $x_N = L$. Introduce the notation for the kernel, which is known for any (n_1, n_2, x_i, x_j) :

$$K_{n_1 n_2}^{ij} = G_{n_1}(x_i - x_j) A_{n_1 n_2}(x_j). \tag{44}$$

Then, a discretization of (43) is

$$\begin{aligned}
\Phi_1(x_i) + \sum_j K_{11}^{ij} \Phi_1(x_j) w_j + \sum_j K_{12}^{ij} \Phi_2(x_j) w_j + \dots + \sum_j K_{1T}^{ij} \Phi_T(x_j) w_j &= f_1(x_i) \\
\Phi_2(x_i) + \sum_j K_{21}^{ij} \Phi_1(x_j) w_j + \sum_j K_{22}^{ij} \Phi_2(x_j) w_j + \dots + \sum_j K_{2T}^{ij} \Phi_T(x_j) w_j &= f_2(x_i) \\
&\vdots \\
\Phi_T(x_i) + \sum_j K_{T1}^{ij} \Phi_1(x_j) w_j + \sum_j K_{T2}^{ij} \Phi_2(x_j) w_j + \dots + \sum_j K_{TT}^{ij} \Phi_T(x_j) w_j &= f_T(x_i)
\end{aligned} \tag{45}$$

where the w_j are precomputed quadrature weights for the nodes x_j . Here, we use trapezoidal quadrature. Each line of the above discretization corresponds to N equations, one for each of the N quadrature nodes. As there are T lines of (45), we have a system of NT equations for NT unknowns.

Rewriting (45) slightly yields

$$\begin{aligned}
\sum_j [(\delta_{ij} + K_{11}^{ij} w_j) \Phi_1(x_j) + K_{12}^{ij} \Phi_2(x_j) w_j + \dots + K_{1T}^{ij} \Phi_T(x_j) w_j] &= f_1(x_i) \\
\sum_j [K_{21}^{ij} \Phi_1(x_j) w_j + (\delta_{ij} + K_{22}^{ij} w_j) \Phi_2(x_j) + \dots + K_{2T}^{ij} \Phi_T(x_j) w_j] &= f_2(x_i) \\
&\vdots \\
\sum_j [K_{T1}^{ij} \Phi_1(x_j) w_j + K_{T2}^{ij} \Phi_2(x_j) w_j + \dots + (\delta_{ij} + K_{TT}^{ij} w_j) \Phi_T(x_j)] &= f_T(x_i).
\end{aligned} \tag{46}$$

We construct a square block matrix B which has size $NT \times NT$. There are T^2 blocks, each of which contains an $N \times N$ matrix. At the (n_1, n_2) block, the (i, j) entry is

$$B^{ij} = \delta_{ij} \delta_{n_1 n_2} + K_{n_1 n_2}^{ij} w_j. \quad (47)$$

Note that $n_1, n_2 = 1, \dots, T$ and $i, j = 1, \dots, N$.

The general system may then be expressed in the block matrix form

$$\mathbf{B}\Phi = \left[I + \begin{pmatrix} \mathbf{K}_{11} & \dots & \mathbf{K}_{1T} \\ \vdots & \ddots & \vdots \\ \mathbf{K}_{T1} & \dots & \mathbf{K}_{TT} \end{pmatrix} \begin{pmatrix} \mathbf{w} & \dots & 0 \\ \vdots & \ddots & \vdots \\ 0 & \dots & \mathbf{w} \end{pmatrix} \right] \Phi = f \quad (48)$$

where

$$\mathbf{w} = \begin{pmatrix} w_1 & \dots & 0 \\ \vdots & \ddots & \vdots \\ 0 & \dots & w_N \end{pmatrix} \quad (49)$$

and

$$\mathbf{K}_{n_1 n_2} = \begin{pmatrix} K_{n_1 n_2}^{11} & \dots & K_{n_1 n_2}^{1N} \\ \vdots & \ddots & \vdots \\ K_{n_1 n_2}^{N1} & \dots & K_{n_1 n_2}^{NN} \end{pmatrix}. \quad (50)$$

The solution $\Phi_n(x_i)$ is computed by numerically solving (48), e.g., by using the backslash operator in MATLAB. With this solution in hand, we compute probabilities of change of state of the confined particle via (35) and (36).

5 Calculation of state change probabilities

Here we present the structure of state change probabilities in a variety of cases. Throughout the section, we take the special case $m_1 = m_2 := m$, i.e., both particles have equal mass.

5.1 Dimensionless quantities

Here we introduce a set of dimensionless quantities with which to characterize this problem. These will guide the numerical experiments that follow. The characteristic unit of mass is m , the unit of length is L , and the unit of time is $T = mL^2/\hbar$, so that $\hbar = 1$ in these units. Then, a unit of energy is $E_U = \hbar/T = \hbar^2/(mL^2)$.

The dimensionless energy of the incident particle is then

$$\tilde{E} = \frac{E}{E_U} = \frac{mL^2 E}{\hbar^2} = L^2 k_0^2 \quad (51)$$

and the dimensionless interaction strength is

$$g = \frac{mL\mu_0}{\hbar^2}. \quad (52)$$

The third dimensionless parameter is n_0 , the stationary state of the confined particle in the incoming state.

We may then define the dimensionless quantity

$$\epsilon = \frac{g}{\sqrt{\tilde{E}}} = \frac{g}{Lk_0} = \frac{m\mu_0}{k_0\hbar^2}, \quad (53)$$

which encodes the strength of the interaction relative to the dimensionless wavenumber of the incident particle. This quantity will be useful to characterize the numerical experiments that follow.

We will explore the effects of varying the dimensionless interaction strength g , the dimensionless wavenumber Lk_0 , and the initial stationary state n_0 on the probabilities of change of state of the confined particle. Unless stated otherwise, we use $T = 50$ truncation terms and $N = 2T$ grid points in a given numerical discretization.

In the tableaux that follow, we plot all possible outcome probabilities p_n (total probability that the interaction leaves particle 2 in eigenstate n), p_n^- (probability that the interaction leaves particle 2 in eigenstate n and particle 1 exits to the left), and p_n^+ (probability that the interaction leaves particle 2 in eigenstate n and particle 1 exits to the right) against incident dimensionless wavenumbers $Lk_0 \in (0, 30)$ of particle 1. We use 500 evenly spaced values of Lk_0 within this interval, with each value of Lk_0 corresponding to a distinct numerical solve of (48). Each figure comprises six panels, all of which involve the confined particle lying in a particular energy state n_0 prior to the interaction. Within each figure, panels (a-c) are associated with $\epsilon > 0$, i.e., a repulsive potential, while panels (d-f) are associated with $\epsilon < 0$, i.e., the equal and opposite attractive potential. In each panel, all possible outcomes are shown except for those associated with $n = n_0$, i.e., we only display outcomes which involve a change in the confined particle's energy state. As discussed earlier, there are only finitely many outcomes available for a given value of Lk_0 .

5.2 Probability structure in the case $n_0 = 1$

We assign the confined particle to be in the ground state prior to the interaction – that is, we fix $n_0 = 1$. We show the structure of available outcomes for high (Fig. 1), moderate (Fig. 2), and low (Fig. 3) interaction strengths.

Fig. 1 displays results for a high interaction strength with $g \sim \mathcal{O}(10^4)$. Correspondingly, the parameter ϵ , which encodes the relative interaction strength, is quite high, and ranges from $\epsilon \sim \mathcal{O}(10^3)$ to $\epsilon \sim \mathcal{O}(10^5)$.

We report several comments and observations regarding Fig. 1. First, further increasing the strength of the interaction (by increasing g) even by several orders of magnitude does not appreciably affect the results of Fig. 1: these represent the limiting high-strength interaction case. Also, perhaps unsurprisingly due to the high interaction strength, the overall probability of reflection (panels b,e) is several orders of magnitude larger than that of transmission (panels c,f). Next, we note that the number of available outcomes, indexed by n , increases for higher Lk_0 . These outcomes grow rapidly yet continuously. Finally, and less intuitively, the structure of outcome probabilities is identical in the repulsive case (panels a-c) as in the attractive case (panels d-f).

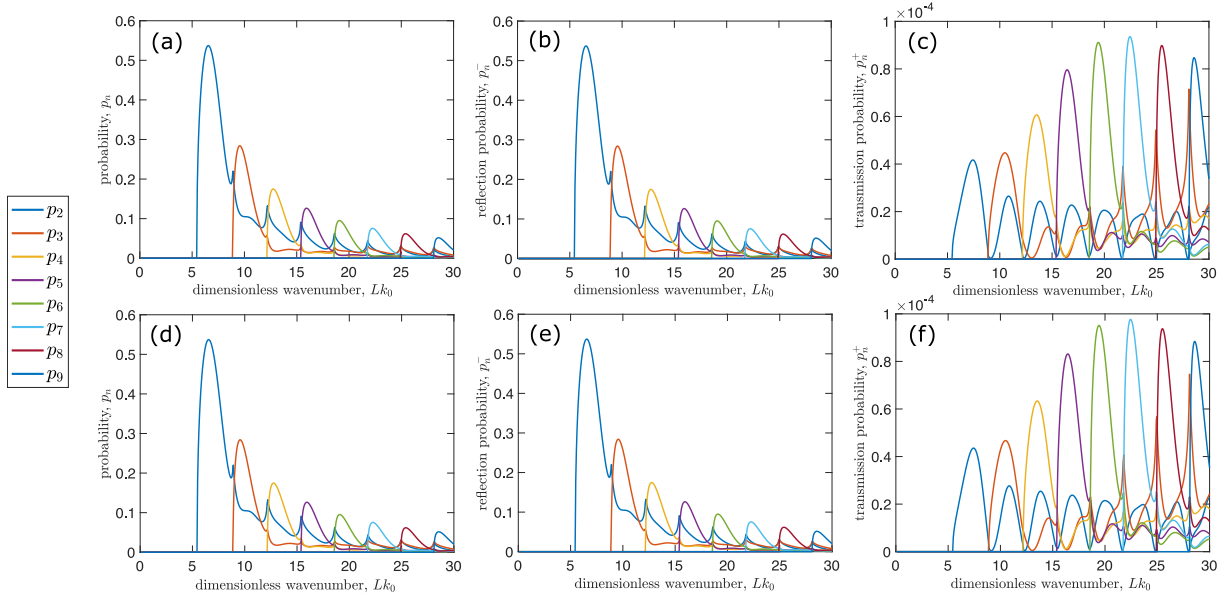


Figure 1: Probability structure with $n_0 = 1$ and a high interaction strength. The parameter ϵ ranges from $\mathcal{O}(10^3) - \mathcal{O}(10^5)$. (a-c) are associated with repulsive interaction, and (d-f) are associated with attractive interaction. (a,d) represent total probabilities indexed by the outcome n ; (b,e) represent reflection probabilities indexed by n ; and (c,f) represent transmission probabilities indexed by n .

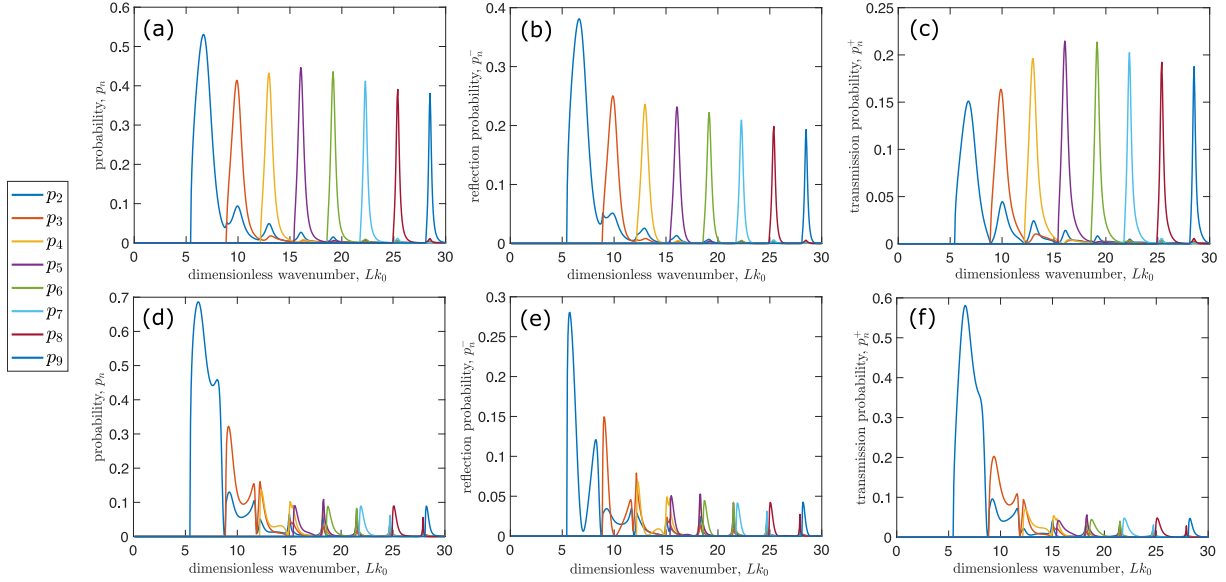


Figure 2: Probability structure with $n_0 = 1$ and a moderate interaction strength. The parameter ϵ ranges from $\mathcal{O}(0.1) - \mathcal{O}(10)$. (a-c) are associated with repulsive interaction, and (d-f) are associated with attractive interaction. (a,d) represent total probabilities indexed by the outcome n ; (b,e) represent reflection probabilities indexed by n ; and (c,f) represent transmission probabilities indexed by n .

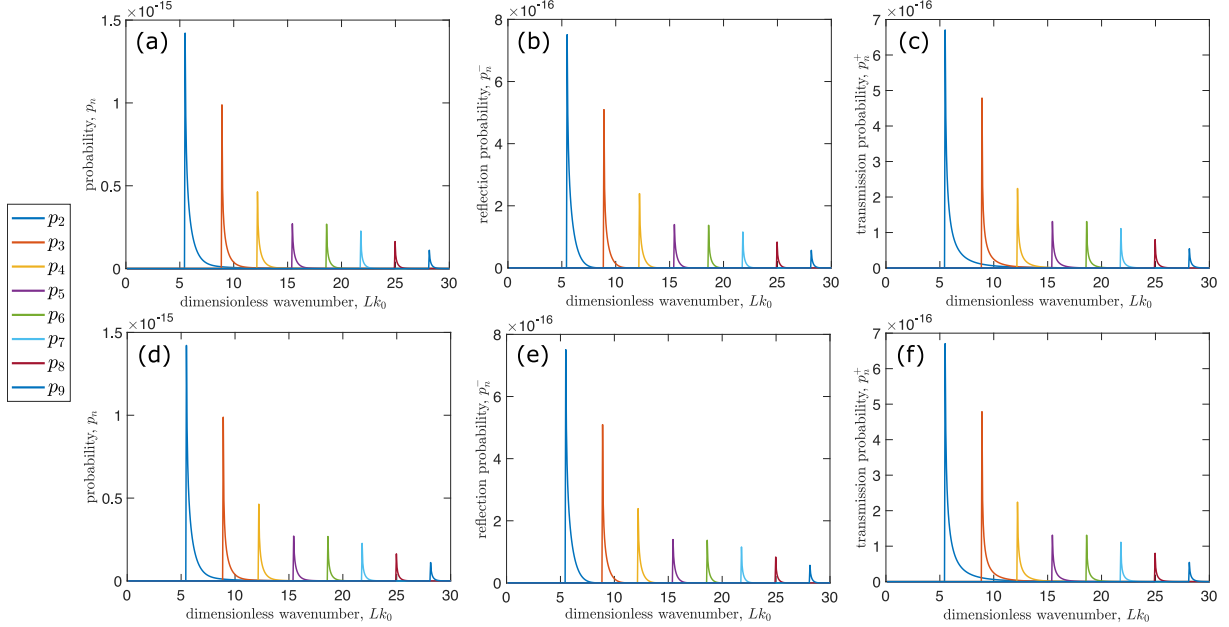


Figure 3: Probability structure with $n_0 = 1$ and a weak relative interaction strength. The parameter ϵ ranges from $\mathcal{O}(10^{-9}) - \mathcal{O}(10^{-7})$. (a-c) are associated with repulsive interaction, and (d-f) are associated with attractive interaction. (a,d) represent total probabilities indexed by the outcome n ; (b,e) represent reflection probabilities indexed by n ; and (c,f) represent transmission probabilities indexed by n .

Fig. 2 displays results in the same format as Fig. 1, with all parameters identical except a decreased $g \sim \mathcal{O}(1)$, which corresponds to a moderate interaction strength. This is associated with $\epsilon \sim \mathcal{O}(0.1)$ to $\epsilon \sim \mathcal{O}(10)$.

Again, we report some observations. In stark contrast to Fig. 1, Fig. 2 displays very different outcomes for a repulsive (panels a-c) versus an attractive (panels d-f) interaction potential. In particular, the attractive potential gives rise to a highly disordered array of outcomes, especially for $Lk_0 \in (7, 20)$. It may be that such choppy behavior is associated with quasi-bound states, in which the incident particle is likely to be trapped but still ultimately exits the box with probability 1. Also, the probability of reflection exceeds that of transmission in the repulsive case, but the opposite is true in the attractive case. Finally, compared to the peaks of Fig. 1, the peaks of Fig. 2 are markedly sharper and narrower (although still continuous).

Fig. 3 displays results in the same format as Figs. 1 and 2, with all parameters identical except a further decreased $g \sim \mathcal{O}(10^{-8})$, i.e., a low interaction strength. This is associated with $\epsilon \sim \mathcal{O}(10^{-9})$ to $\epsilon \sim \mathcal{O}(10^{-7})$. Just as in the high interaction strength case, we report that the very low interaction results are essentially unchanged (up to the scaling factor ϵ^2) as the interaction strength is decreased further. Also similarly to the high interaction strength case (Fig. 1), the attractive and repulsive results are identical; these only differ in the moderate interaction strength case (Fig. 2). Finally, we note that the peaks of probability display a highly regular pattern, with a peak for a given outcome

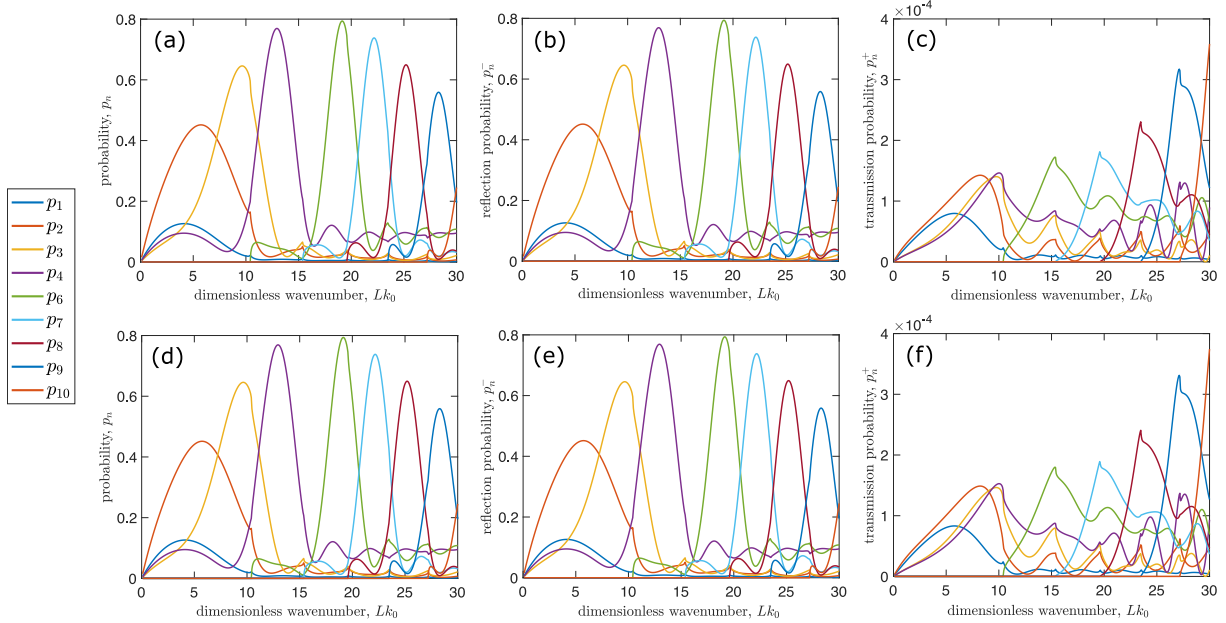


Figure 4: Probability structure with $n_0 = 5$ and a high interaction strength. The parameter ϵ ranges from $\mathcal{O}(10^3) - \mathcal{O}(10^5)$. (a-c) are associated with repulsive interaction, and (d-f) are associated with attractive interaction. (a,d) represent total probabilities indexed by the outcome n ; (b,e) represent reflection probabilities indexed by n ; and (c,f) represent transmission probabilities indexed by n .

n arising sharply and then decaying rapidly in a narrow range of Lk_0 .

5.3 Probability structure in the case $n_0 = 5$

We now assign the confined particle to be in a higher-energy stationary state prior to the interaction – that is, we fix $n_0 = 5$. We repeat the experiments of the previous section and show results for high (Fig. 4), moderate (Fig. 5), and low (Fig. 6) interaction potentials.

The results for $n_0 = 5$ largely mirror those of $n_0 = 1$. That is, for very high interaction strengths, i.e., large ϵ (Fig. 4), as well as for very weak interaction strengths, i.e., small ϵ (Fig. 6), the probability structure is identical in the repulsive and attractive cases. Only the moderate- ϵ case (Fig. 5) exhibits different outcomes for attractive and repulsive interactions. Another similarity between the cases $n_0 = 1$ and $n_0 = 5$ is that very strong potentials render the probability of transmission to be several orders of magnitude lower than that of reflection – no matter the state of the confined particle, the incident particle is generally unlikely to exit to the right when the interaction is very strong.

The effect of possible quasi-bound states is again visible in the attractive, moderately strong interaction potential case of Fig. 5(c-f). Sharp peaks arise and the structure of p_n is highly irregular.

The overall structure for $n_0 = 5$ is significantly more complex than that for $n_0 = 1$; the confined particle's energy may decrease or increase depending on Lk_0 . Outcomes in which

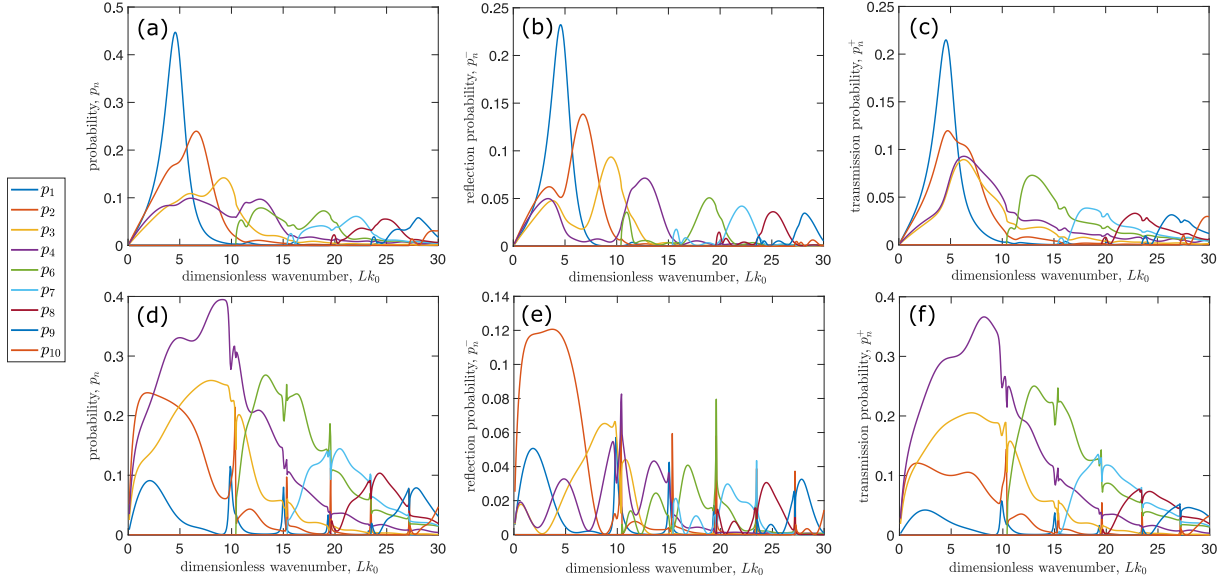


Figure 5: Probability structure with $n_0 = 5$ and a moderate interaction strength. The parameter ϵ ranges from $\mathcal{O}(0.1) - \mathcal{O}(10)$. (a-c) are associated with repulsive interaction, and (d-f) are associated with attractive interaction. (a,d) represent total probabilities indexed by the outcome n ; (b,e) represent reflection probabilities indexed by n ; and (c,f) represent transmission probabilities indexed by n .

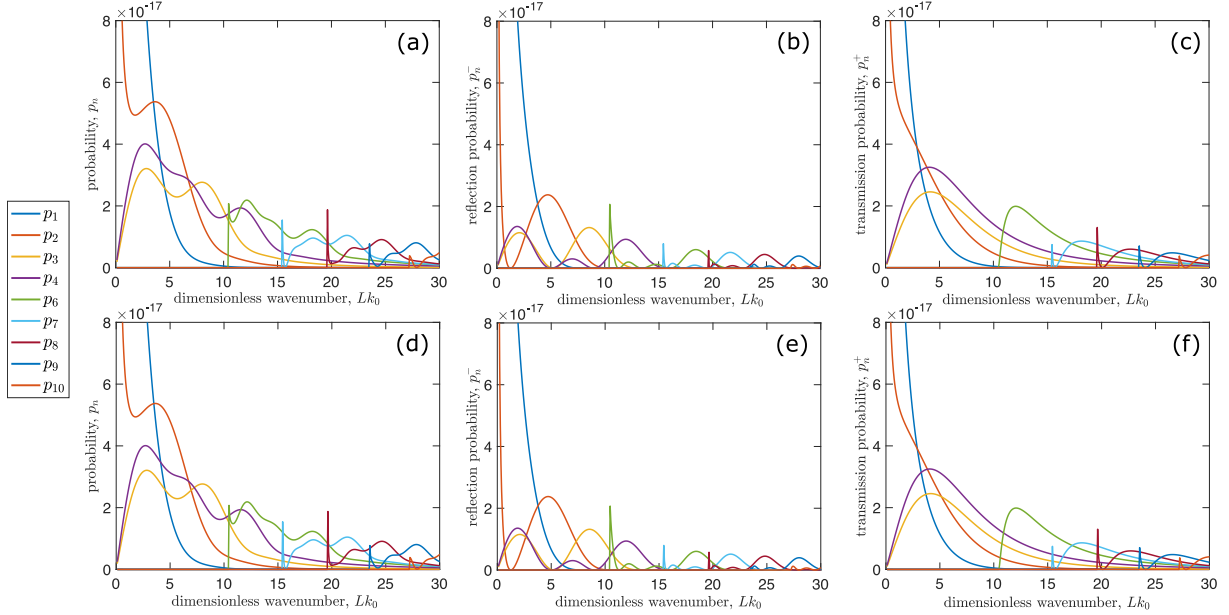


Figure 6: Probability structure with $n_0 = 5$ and a low interaction strength. The parameter ϵ ranges from $\mathcal{O}(0.1) - \mathcal{O}(10)$. (a-c) are associated with repulsive interaction, and (d-f) are associated with attractive interaction. (a,d) represent total probabilities indexed by the outcome n ; (b,e) represent reflection probabilities indexed by n ; and (c,f) represent transmission probabilities indexed by n .

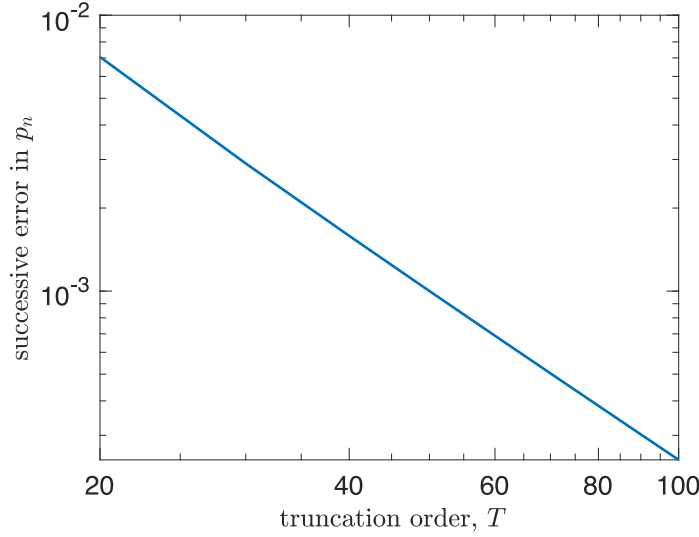


Figure 7: Second-order convergence of numerical method. Arbitrarily chosen parameters $Lk_0 = 20$ and $g = 80$ are fixed, and the number of mesh points N varies with the truncation order T by $N = 2T$. Successive refinement in T yields second-order convergence.

the confined particle loses energy arise for even very small Lk_0 , whereas if the particle begins in the ground energy state with $n_0 = 1$, there is a range of small Lk_0 for which the particle remains in the ground state with probability 1.

6 Convergence of numerical method

Here we demonstrate that the numerical method presented to solve (20) exhibits second-order convergence with respect to simultaneous refinement in the truncation order T and the number of mesh points N . We arbitrarily fix $Lk_0 = 20$ and $g = 80$, so that $\epsilon = \mathcal{O}(10)$, and compute the set of probabilities of all possible outcomes p_n for $T = 10, 20, \dots, 100$. We relate N to T via $N = 2T$. We then plot the quantity

$$|p_n^{i+1} - p_n^i|, \quad i = 1, \dots, 9 \quad (54)$$

against T on a log-log plot in Fig. 7. The slope of the line is -2.08 , which confirms second-order convergence of the numerical method.

7 Summary and conclusions

In this paper, we have considered the one-dimensional scattering of a free particle against a confined particle, in which the two particles interact via a delta-function potential which may be repulsive or attractive. The confined particle is restricted to move in the interval $(0, L)$, while the space available to the free particle is the whole real line, and the boundaries $x = 0$ and $x = L$ are transparent to the free particle.

Starting from the time-independent Schrodinger equation, we have derived an infinite system of integral equations, which we have solved numerically by truncation and discretization. The computational results show that the method is second-order accurate.

We have considered an incoming product state in which the free particle is incident from the left with prescribed energy, and the confined particle is in one of the possible stationary states of a particle in a one-dimensional box. We have calculated the probabilities of the finitely many possible outcomes, each of which corresponds to the confined particle being in some (possibly different) stationary state of a particle in a one-dimensional box, and the free particle flying out to the right or left with some definite energy. It is a direct consequence of conservation of energy that there are only finitely many possible outcomes. In some of these outcomes, the free particle loses energy and the particle in the box moves up by one or more energy levels, but this is only possible if the free particle has sufficient incoming energy. In other outcomes, the free particle stimulates a loss of energy of the confined particle, provided that the confined particle was not in its ground state initially.

We have presented computational results which show how the probabilities of these discrete outcomes depend on the dimensionless wavenumber of the free particle for low, moderate, and high delta-potential interaction strengths, in both the attractive and repulsive cases. These representative examples cover two types of cases: one with the confined particle initially in its ground state, $n_0 = 1$, and another with the confined particle initially in an excited state, specifically $n_0 = 5$.

An important motivation of this work has been to understand the nature of state change in quantum mechanics. Since understanding is subjective, only the reader can decide whether or not we have been successful in this goal. In the process, however, we have developed a general non-perturbative framework that can be used to calculate the probabilities of different outcomes in one-dimensional scattering. Whether this framework can be of use, for example in the study of quantum wires [5, 1] and quantum dots [2, 3], remains to be seen.

Acknowledgments

We thank Michael Weinstein for helpful discussions.

References

- [1] LI Goncharov, AM Yafyasov, and DE Tsurikov. A semispectral approach for the efficient calculation of scattering matrices in quasi-1D quantum systems and transmission coefficients for the Landauer formula. *Journal of Computational Electronics*, 13:885–893, 2014.
- [2] Lucjan Jacak, Pawel Hawrylak, and Arkadiusz Wojs. *Quantum dots*. Springer Science & Business Media, 2013.

- [3] Leo Kouwenhoven and Charles Marcus. Quantum dots. *Physics World*, 11(6):35, 1998.
- [4] A Soffer and Michael I Weinstein. Nonautonomous Hamiltonians. *Journal of statistical physics*, 93:359–391, 1998.
- [5] JY Vaishnav, A Itsara, and EJ Heller. Hall of mirrors scattering from an impurity in a quantum wire. *Physical Review B—Condensed Matter and Materials Physics*, 73(11):115331, 2006.